Electronic Supplementary Material (ESI) for RSC Advances.

SUPPLEMENTARY INFORMATION

Novel hydrogen- and halogen-bonding anion receptors based on 3-iodopyridinium units

Valeria Amendola,[a]* Greta Bergamaschi,[a] Massimo Boiocchi,[b] Nadia Fusco,[a] Vincenzo Mario La Rocca,[c] Laura Linati,[b] Eliana Lo Presti,[a] Massimo Mella,[c]* Pierangelo Metrangolo[d]* and Ana Miljkovic[a]

a. *Department of Chemistry, Università degli Studi di Pavia, via Taramelli 12, Pavia (Italy).*
b. *Centro Grandi Strumenti, via Ferrata, Pavia (Italy); amendola@unipv.it*
c. *Dipartimento di Scienza ed Alta Tecnologia, Universita' degli Studi dell'Insubria, via Valleggio 11, 22100 Como (Italy); massimo.mella@uninsubria.it*
d. *Department of Chemistry, Materials and Chemical Engeneering, Politecnico di Milano, via Mancinelli 7, Milano (Italy); pierangelo.metrangolo@polimi.it*

Index:

1. Syntheses

1.1 Synthesis of 1a(PF_6)

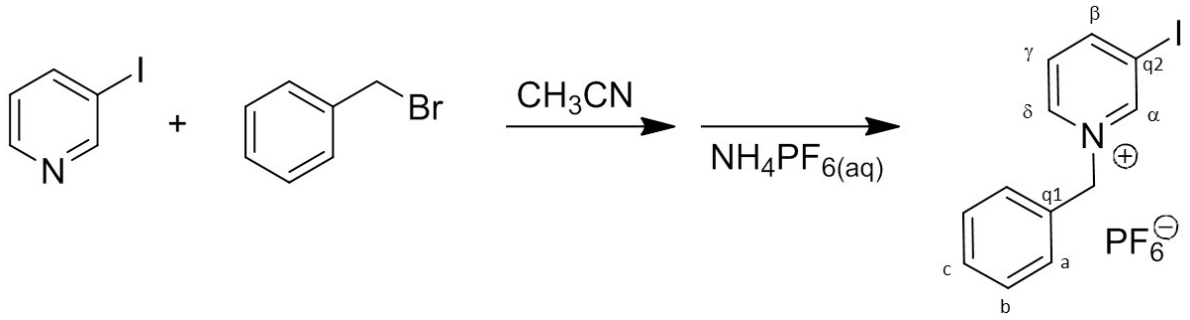

To a solution of 3-iodopyridine (0.10 g, 0.49 mmol) in acetonitrile (10mL), an acetonitrile solution of benzyl bromide (0.10 g, 0.58 mmol, in 10 mL) was added under stirring. The mixture was refluxed for 72 hrs. The solvent was then evaporated to dryness, and the solid residue was washed with dichloromethane and filtered. The final product was then isolated as an hexafluorophosphate salt by dissolving the solid in warm water, and treating it with a saturated solution of NH_4PF_6(aq). The white solid was collected and dried. Yield: 71%

$C_{12}H_{11}NIPF_6$: found: C, 32.62; H, 2.56; N, 3.16%, calculated: C, 32.68; H, 2.51; N, 3.18%

ESI–MS, MeOH (m/z): 296.15 [**1a**]$^+$.

^{1}H–NMR (400 MHz), d^6–DMSO (ppm): 9.65 (s, Hα, 1H), 9.15 (d, Hβ, 1H), 8.97 (d, Hδ, 1H), 7.93 (t, Hγ, 1H), 7.51 (d, Hb, 2H), 7.49 (m, Hc-d, 3H), 5.44 (s, CH_2, 2H).

^{13}C–NMR (400 MHz), d^6–DMSO (ppm): 155.94 (Cβ), 151.67 (Cα), 145.09 (Cδ), 134.01 (q1), 131.69 (Cc), 131.14 (Ca), 130.97 (Cb), 130.66 (Cγ), 95.71 (q2), 66.23 (CH_2).

1.2 Synthesis of 2(PF_6)$_3$

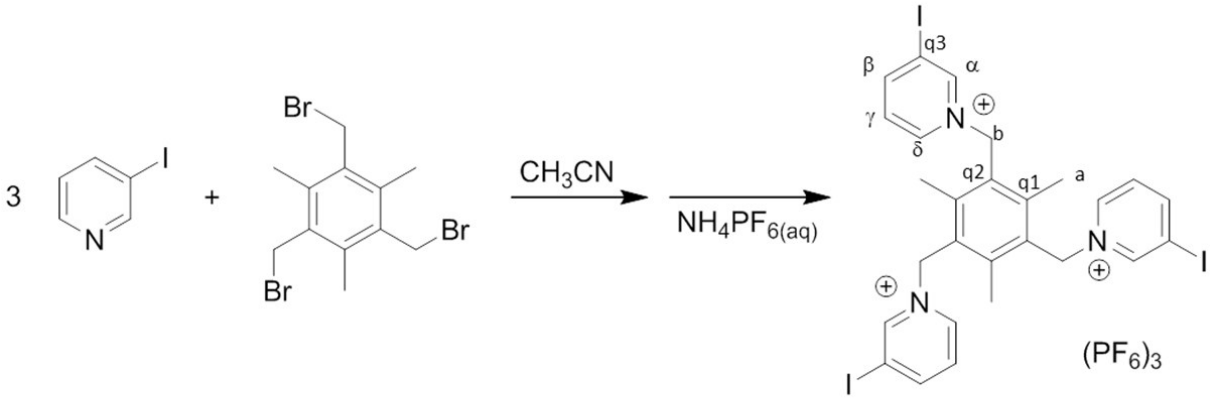

To a solution of 3-iodopyridine (0.19 g, 0.93 mmol) in acetonitrile (5 mL), an acetonitrile solution of 1,3,5-tribromomethyl mesitylene (0.10 g, 0.25 mmol, in 7 mL) was added under stirring. The mixture was refluxed

for 72 hrs. The solvent was then evaporated to dryness, and the solid residue was washed with dichloromethane and filtered. The final product was then isolated as an hexafluorophosphate salt by dissolving the solid in warm water, and treating it with a saturated solution of NH_4PF_6(aq). The white solid was collected and dried. Yield: 62%

$C_{27}H_{27}N_3I_3P_3F_{18}$: found: C, 26.65; H, 2.32; N, 3.40%, calculated: C, 26.82; H, 2.25; N, 3.48%

ESI–MS, MeOH (m/z): 258.50 $[\mathbf{2}]^{3+}$, 459.94 $[\mathbf{2} + PF_6^-]^{2+}$.

^{1}H–NMR (400 MHz), d^6–DMSO (ppm): 9.42 (s, Hα, 3H), 8.99 (d, Hβ, 3H), 8.52 (d, Hδ, 3H), 7.83 (t, Hγ, 3H), 5.99 (s, Hb, 6H), 2.24 (s, Ha, 9H).

^{13}C–NMR (400 MHz), d^6–DMSO (ppm): 154.97 (Cβ), 151.12 (Cα), 145.49 (q1), 143.34 (Cδ), 131.37 (Cγ), 129.57 (q2), 97.30 (q3), 59.84 (Cb), 18.23 (Ca).

1.3 Synthesis of $3(PF_6)_3$

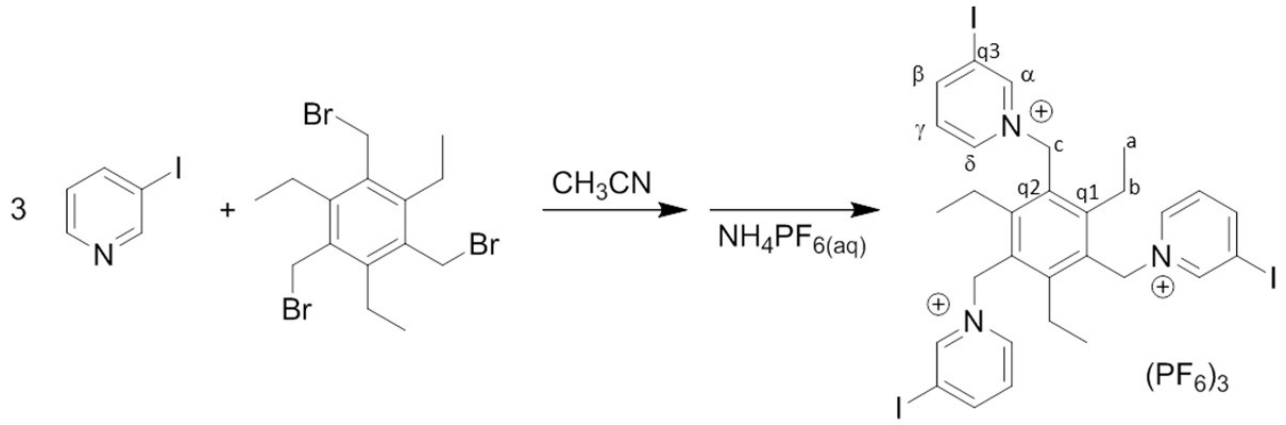

To a solution of 3-iodopyridine (0.19 g, 0.93 mmol) in acetonitrile (5 mL), an acetonitrile solution of 1,3,5–tribromomethyl–2,4,6–triethylbenzene (0.10 g, 0.23 mmol, in 7 mL) was added under stirring. The mixture was refluxed for 72 hrs. The solvent was then evaporated to dryness, and the solid residue was washed with dichloromethane and filtered. The final product was then isolated as an hexafluorophosphate salt by dissolving the solid in warm water, and treating it with a saturated solution of NH_4PF_6(aq). The white solid was collected and dried. Yield: 56%

$C_{30}H_{33}N_3I_3P_3F_{18}$: found: C, 28.67; H, 2.72; N, 3.24%, calculated: C, 28.80; H, 2.66; N, 3.36%

ESI–MS, MeOH (m/z): 272.33 $[\mathbf{3}]^{3+}$, 480.50 $[\mathbf{3} + PF_6^-]^{2+}$.

^{1}H–NMR (400 MHz), d^6–DMSO (ppm): 9.54 (s, Hα, 3H), 9.00 (d, Hβ, 3H), 8.53 (d, Hδ, 3H), 7.84(t, Hγ, 3H), 5.96 (s, Hc, 6H), 2.60 (m, Hb, 6H), 0.77 (t, Ha, 9H).

^{13}C–NMR (400 MHz), d^{6}–DMSO (ppm): 154.98 (Cβ), 151.62 (Cα), 151.52 (q1), 142.96 (Cδ), 130.17 (Cγ), 128.75 (q2), 97.05 (q3), 58.35 (Cc), 24.77 (Cb), 16.28 (Ca).

2. Anion binding studies on the mono-branched receptors

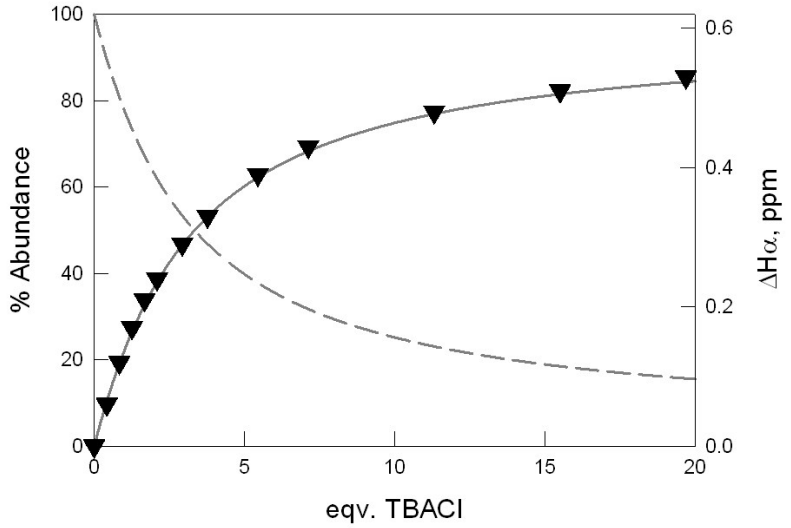

Fig. S1: Family of ^{1}H-NMR spectra and profile for the titration of **1a** (1.85 mM) with TBACl in CD_3CN, superimposed to the distribution diagram built for the formation of a 1:1 complex characterized by LogK_{11} = 2.30(3). The black triangles show the shift of proton Hα vs. equivalents of added chloride.

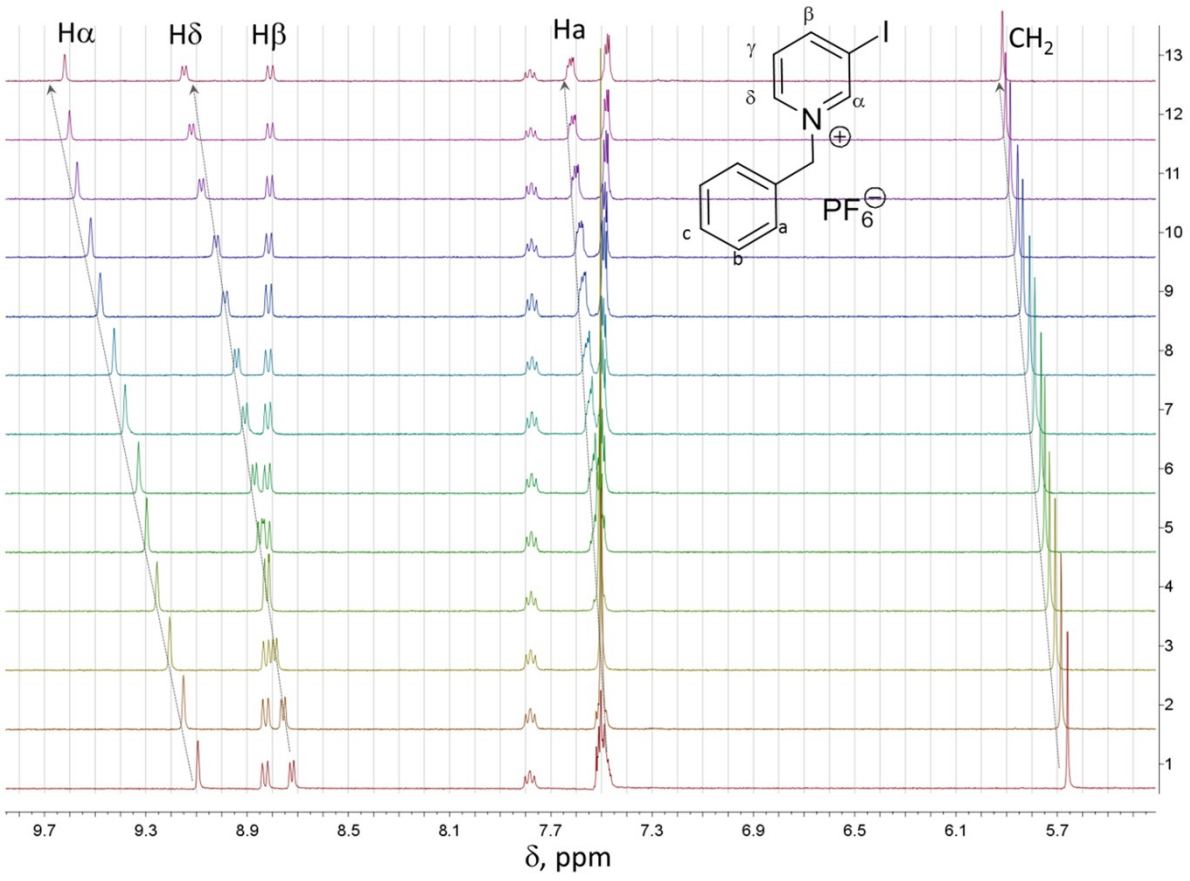

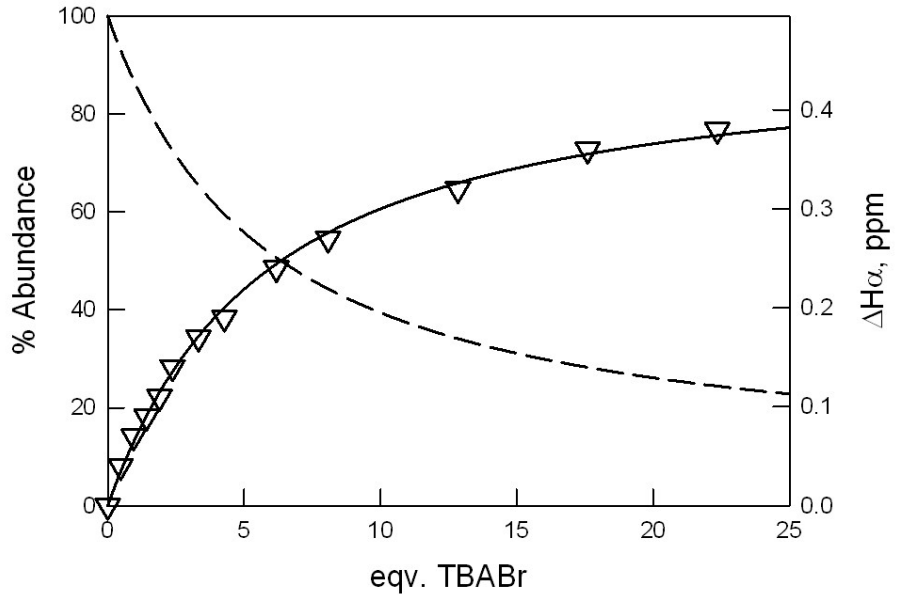

Fig. S2: Family of ^{1}H-NMR spectra and profile for the titration of **1a** (1.85 mM) with TBABr in CD_3CN. The profile (white triangles) shows the shift of protons Hα vs. equivalents of added anion. The profile is superimposed to the distribution diagram built for the formation of a 1:1 complex characterized by LogK_{11} = 1.98(4).

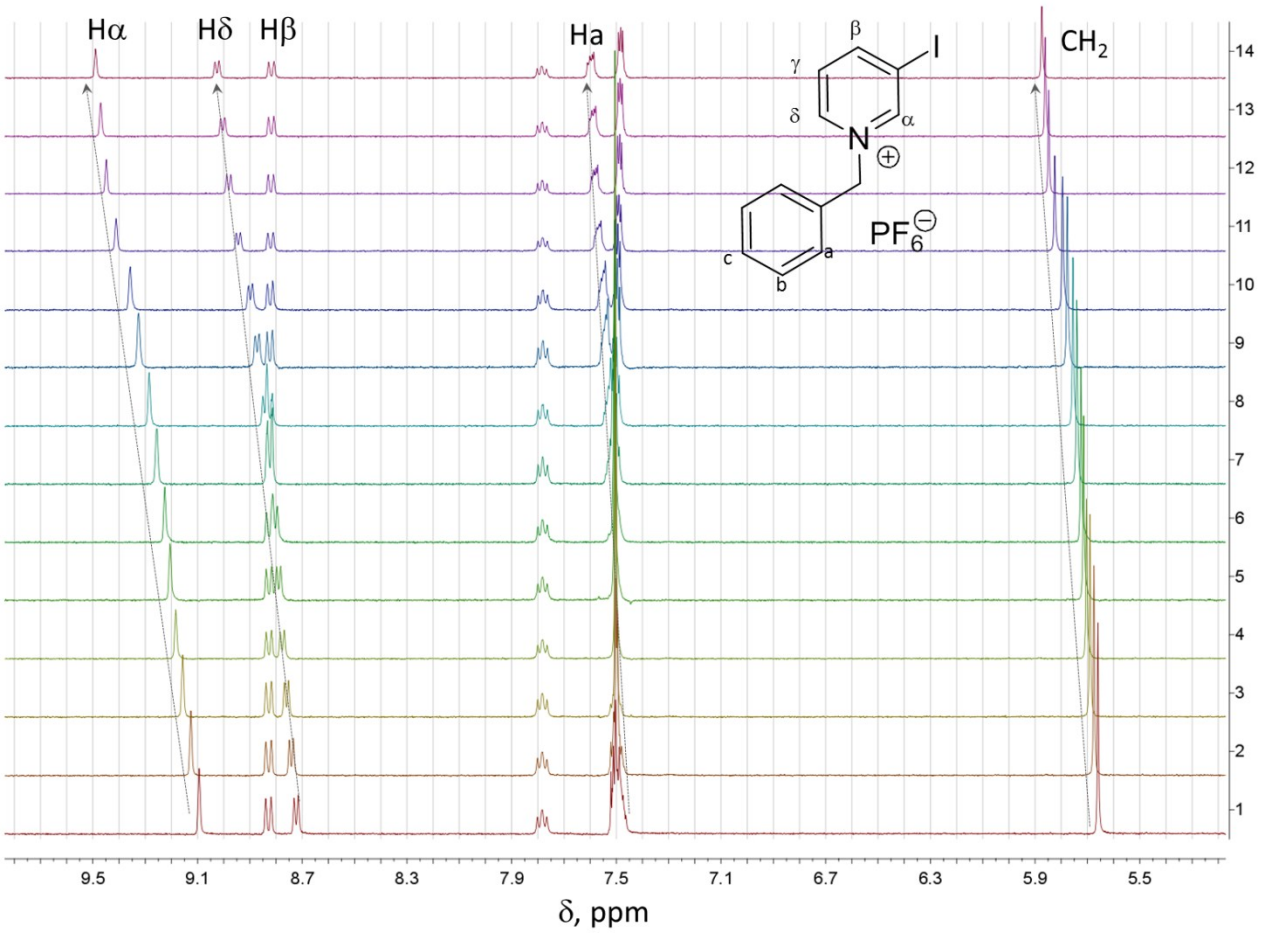

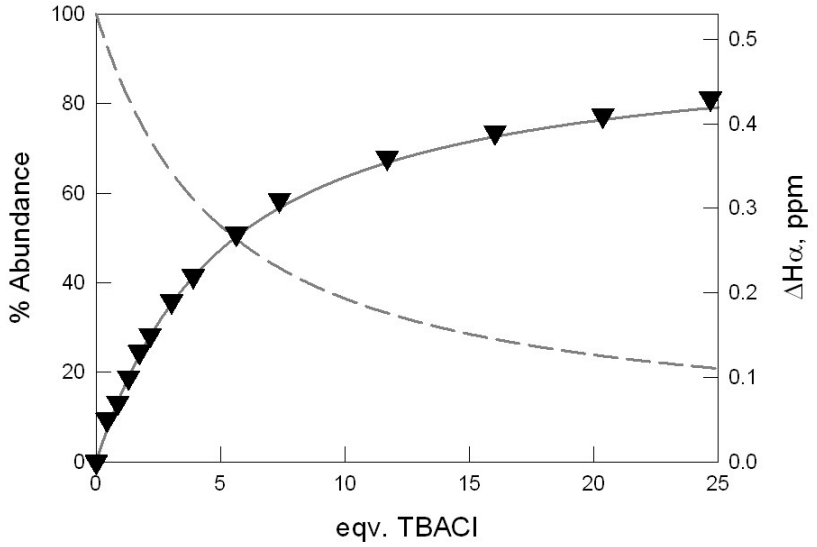

Fig. S3: Family of ^{1}H-NMR spectra and profile for the titration of **1b** (1.85 mM) with TBACl in CD_3CN. The profile (black triangles) shows the shift of protons Hα (in α position to the positively charged nitrogen) vs. equivalents of added chloride. The profile is superimposed to the distribution diagram built for the formation of a 1:1 complex characterized by $\mathrm{Log}K_{11} = 2.06(1)$.

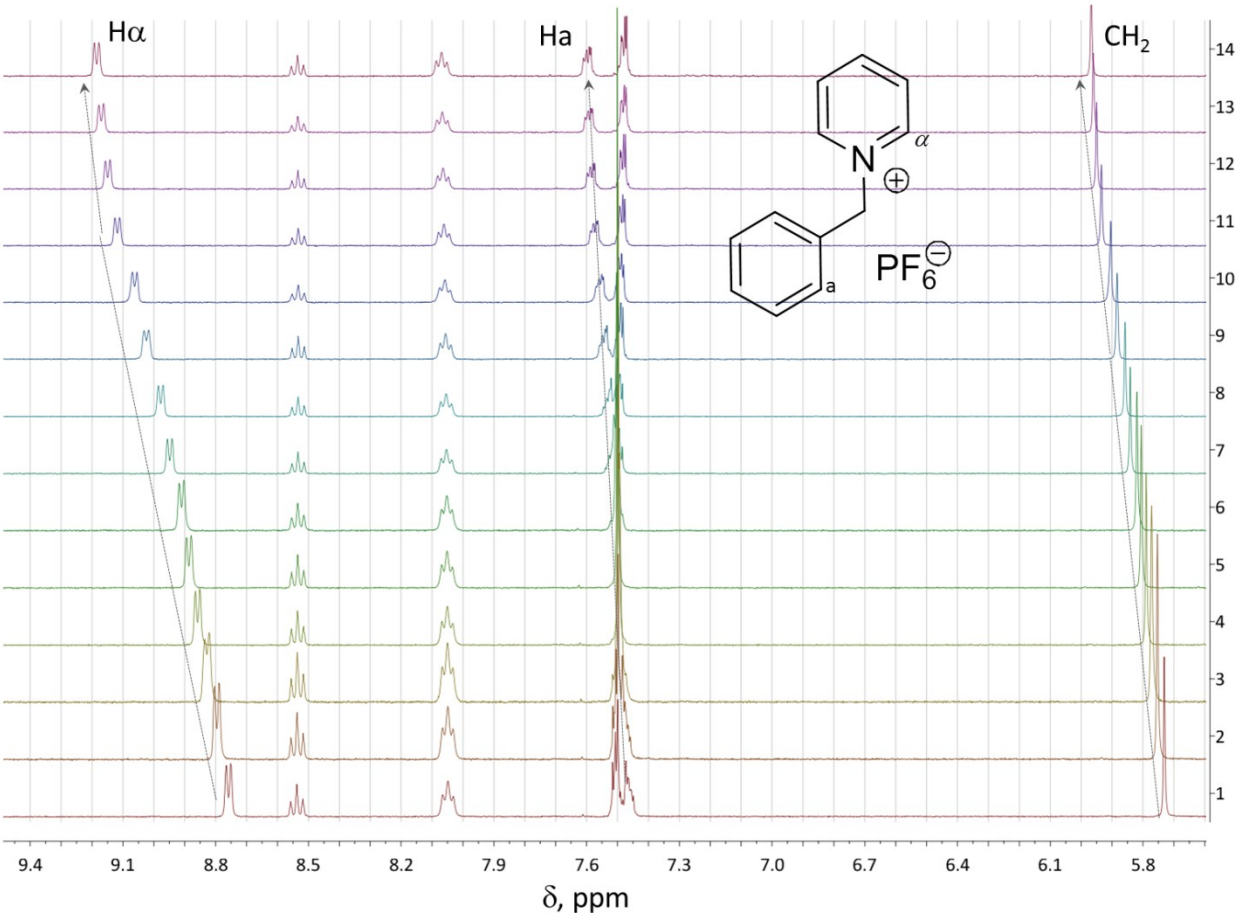

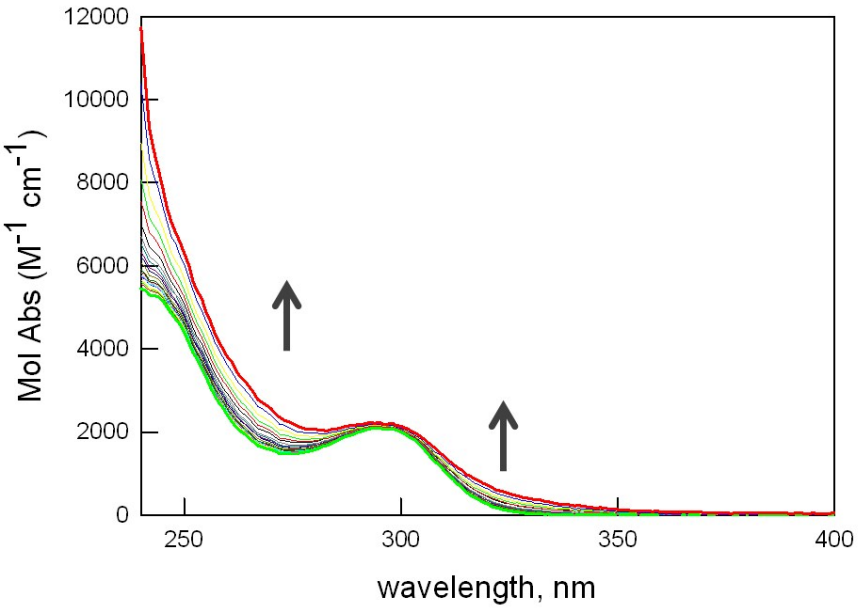

Fig. S4: UV-vis spectra recorded during the titration of **1a** (0.5 mM) with TBACl in acetonitrile.

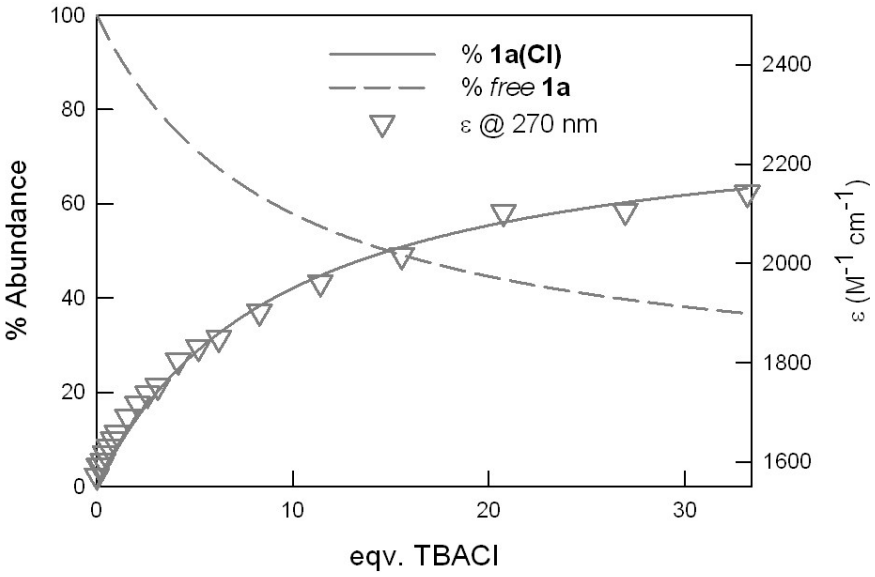

Fig. S5: UV-vis titration profile of **1a(PF_6)** (0.5 mM) with TBACl in acetonitrile, superimposed to the distribution diagram built for the formation of a 1:1 complex characterized by LogK_{11} = 2.27(1). The triangles show the profile of the Mol Abs at 270 nm vs. equivalents of added chloride.

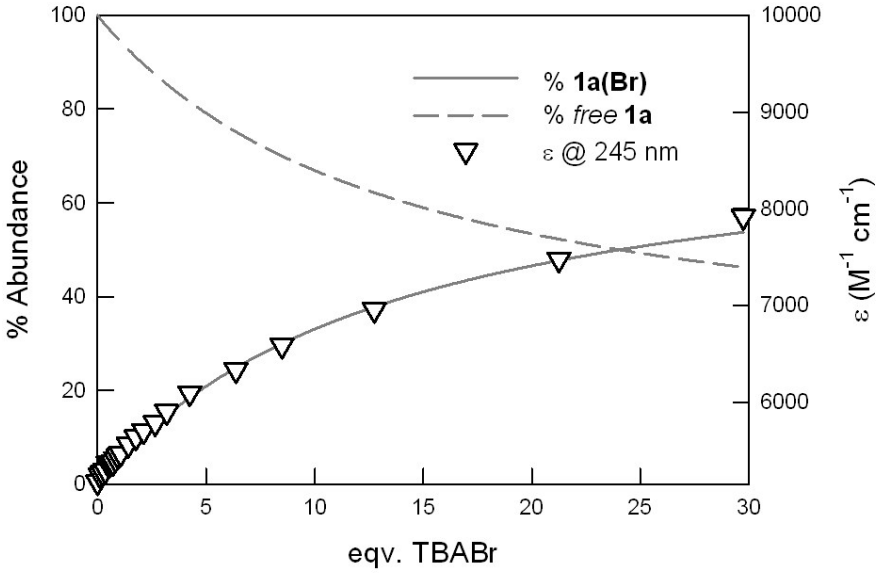

Fig. S6: UV-vis titration profile of **1a(PF_6)** (0.5 mM) with TBABr in acetonitrile, superimposed to the distribution diagram built for the formation of a 1:1 complex characterized by LogK_{11} = 2.08(1). The triangles show the profile of the Mol Abs at 245 nm vs. equivalents of added bromide.

3. Computational studies

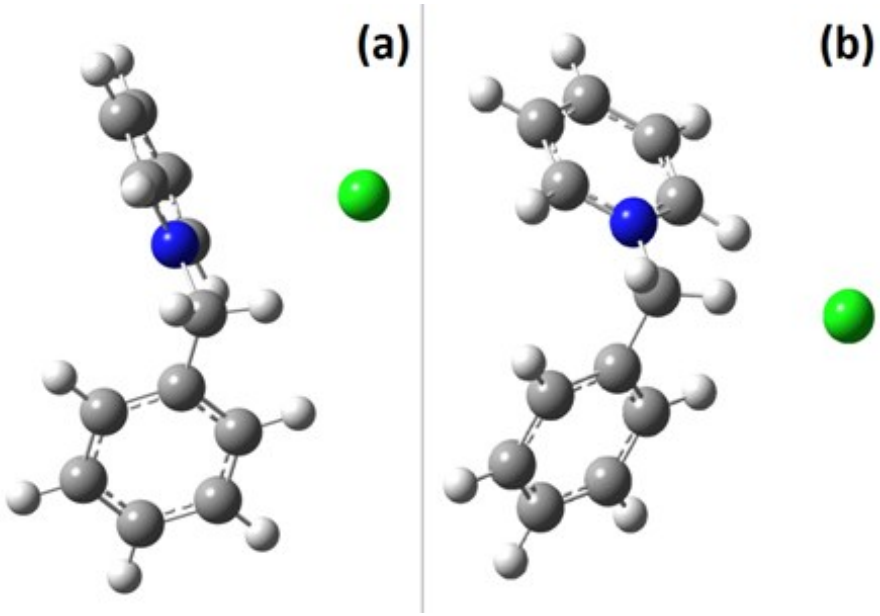

Fig. S7: Geometries of two possible conformers for **1b**$^{+}$/Cl^{-}.

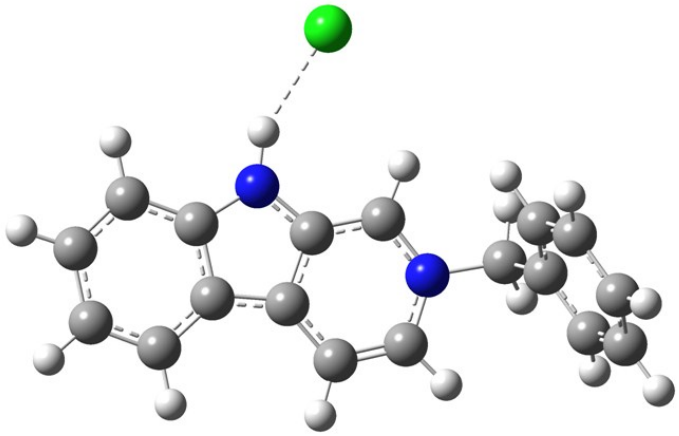

Fig. S8: Optimized structure of the **1a**$^{+}$/Cl^{-} complex, from which it is evidenced the strong HB with Cl^{-}.

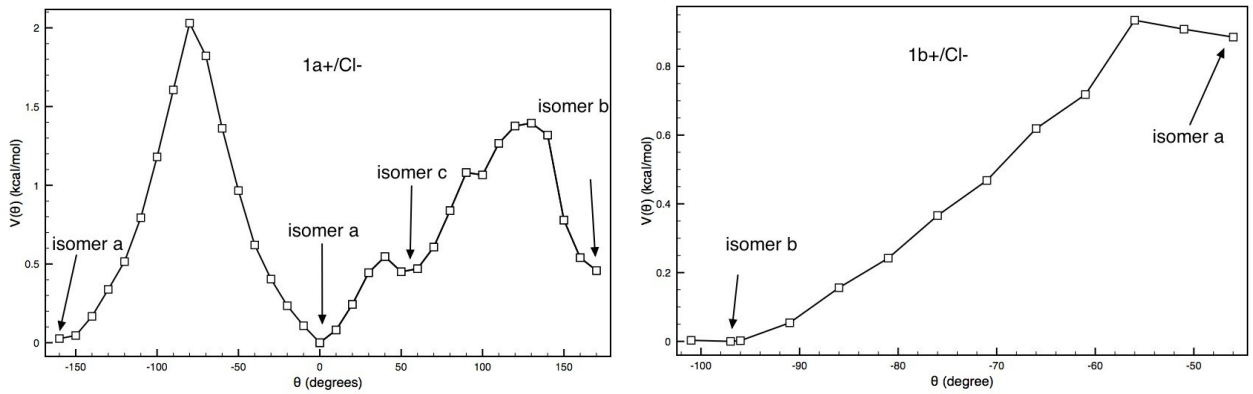

Fig. S9: Relaxed torsional scan around the CH_2-N bond in the **1a**$^+$/Cl$^-$ and **1b**$^+$/Cl$^-$ complexes; the position of the lowest isomers in Figs. 2 (main text) and S7 are also indicated for the sake of clarity.

Comp.	**IPDE** (kcal/mol) **X=Cl**$^-$	**IPDE** (kcal/mol) **X=Br**$^-$	**IPDE** (kcal/mol) **X=I**$^-$
1a	5.65; 5.39 4.93; 4.12	4.84; 4.95 5.07; 3.91	4.58; 4.34 5.12; 4.24
1b	5.22; 4.14	4.15; 4.72	
1c	8.40	7.28	

Tab. S1: Counterpoise corrected IPDE for the species in Table 2 of the main text; the order of the isomers is maintained.

Comp.	**IPDE** (kcal/mol) **X=Cl**$^-$	**IPDE** (kcal/mol) **X=Br**$^-$
2	6.43; 4.88, 6.04; 5.21	7.26; 7.46

Tab. S2: Counterpoise corrected IPDE for the species in Table 6 of the main text; the order of the isomers is maintained.

4. X-Ray diffraction studies on 1a(PF_6)

In the crystal structure of **1a**(PF_6) (see Fig. S10), only a weak HB interaction is present, with the shortest D···A separation of 3.13(1) Å. This distance, involving a C-H bond of the iodopyridinum moiety and a F atom of the counter ion, is only slightly shorter than the sum of Van der Waals radii of C and F atoms: 3.17 Å.[1] Geometrical features for the HB interaction are reported in the manuscript (Table 3).

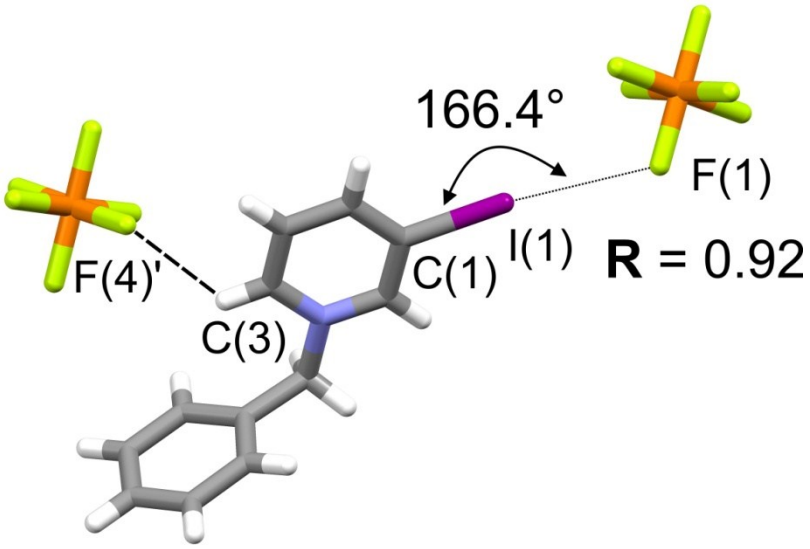

Fig. S10. A simplified sketch of the crystal structure of **1a(PF_6)**. Atom names are shown only for atom involved in C-I···Y halogen bonds (drawn with dotted lines) and weak C-H···A hydrogen bonds (drawn with dashed lines). The normalized **R** values = dI···Y/(rI+rY) and the C-I···Y bond angle are reported. Symmetry code: (') = -1+x, 1/2-y, -1/2+z; (") =1+x, y, z.

A weak XB interaction could be also noted, between the C-I group of the iodopyridinum (XB-donor) and a F atom of PF_6– (XB-acceptor). Also in this case, the I···F distance [i.e. 3.18(1)Å] is shorter than the sum of the Van der Waals radii for I and F atoms: 3.45 Å;[1] (see Table 4 in the manuscript). However, the normalized value **R** [defined as the ratio between the observed I···F separation and the sum of their Van der Waals radii] is only 0.92, and the C-I···F angle is 166.4(3)°, i.e. far from the linear values expected for a typical R-X···Y halogen bond.[2] In conclusion, the crystal structure of **1a(PF_6)** suggests that only weak HB and XB interactions occur between the **1a**$^+$ molecular cation and the PF_6^- anion.

5. Anion binding studies on the tripodal receptors

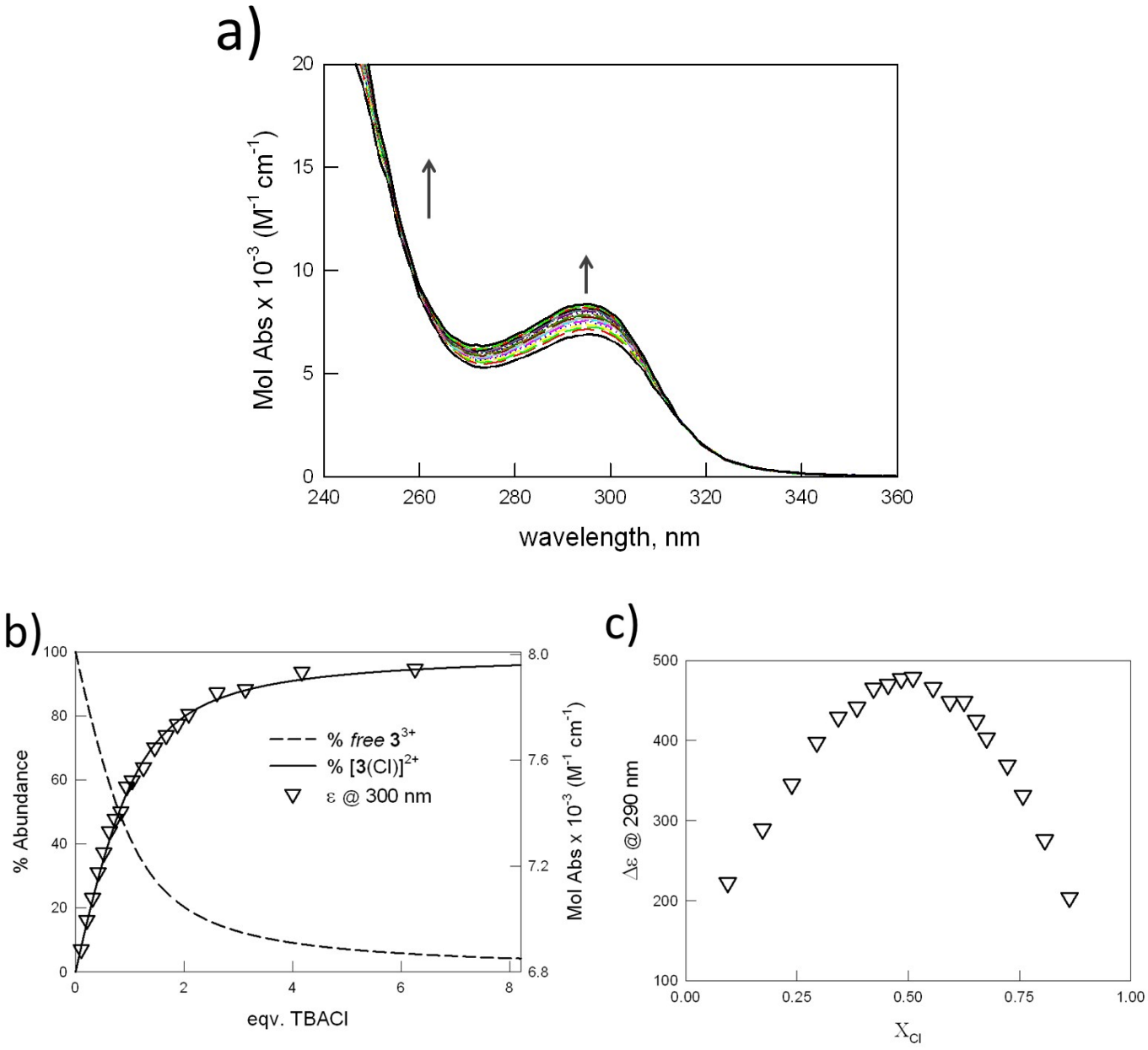

Fig. S11. a) UV-vis spectra recorded during the titration of **3(PF$_6$)$_3$** (0.02 mM) with TBACl (20°C) in pure acetonitrile. b) Titration profile at 300 nm, superimposed to the distribution diagram built for the formation of a 1:1 complex, LogK_{11} = 5.16(1). c) Job plot at 290 nm.

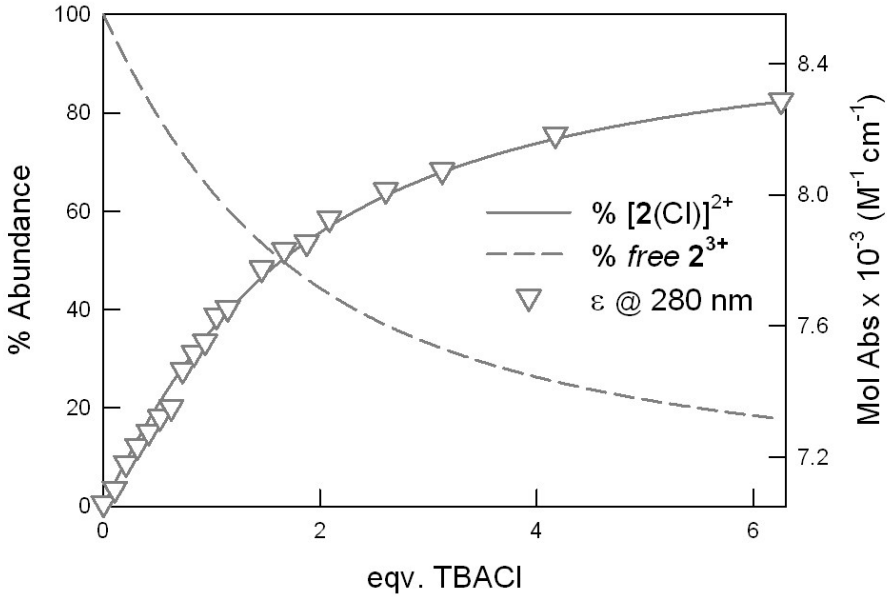

Fig. S12: UV-vis titration profile of **2(PF$_6$)$_3$** (0.02 mM) with TBACl (20°C) in pure acetonitrile, superimposed to the distribution diagram built for the formation of a 1:1 complex characterized by LogK_{11} = 4.65(1). The triangles show the profile of the Mol Abs at 280 nm vs. equivalents of added chloride.

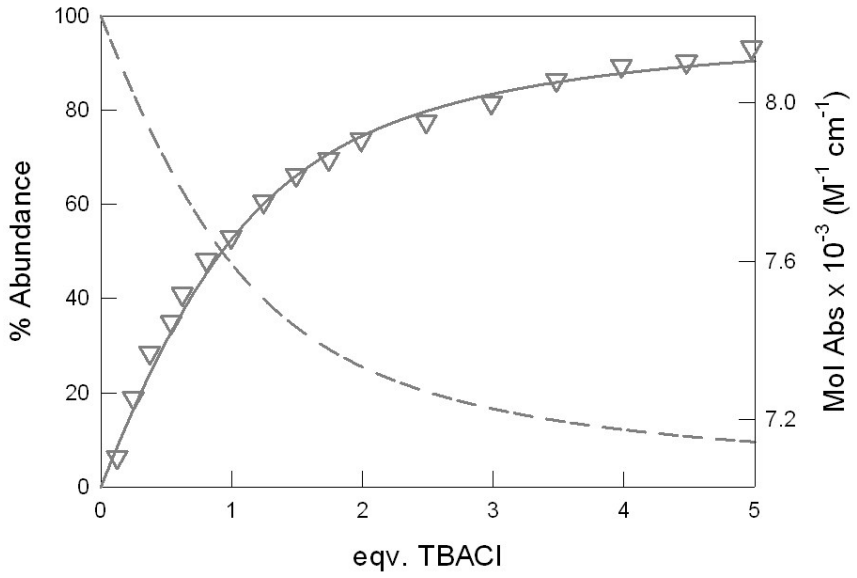

Fig. S13: UV-vis spectra and titration profile of **3(PF$_6$)$_3$** (0.2 mM) with TBACl in acetonitrile/DMSO mixture (10% DMSO), superimposed to the distribution diagram built for the formation of a 1:1 complex characterized by LogK_{11} = 4.07(2). The triangles show the profile of the Mol Abs at 300 nm vs. equivalents of added chloride.

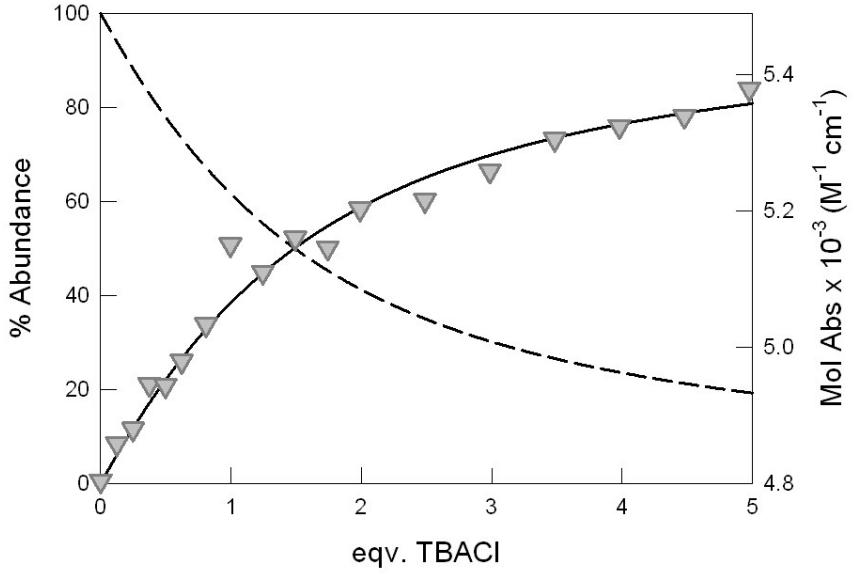

Fig. S14: UV-vis titration profile of **2(PF$_6$)$_3$** (0.2 mM) with TBACl in acetonitrile/DMSO mixture (10% DMSO), superimposed to the distribution diagram built for the formation of a 1:1 complex characterized by LogK_{11} = 3.70(2). The triangles show the profile of the Mol Abs at 311 nm vs. equivalents of added chloride.

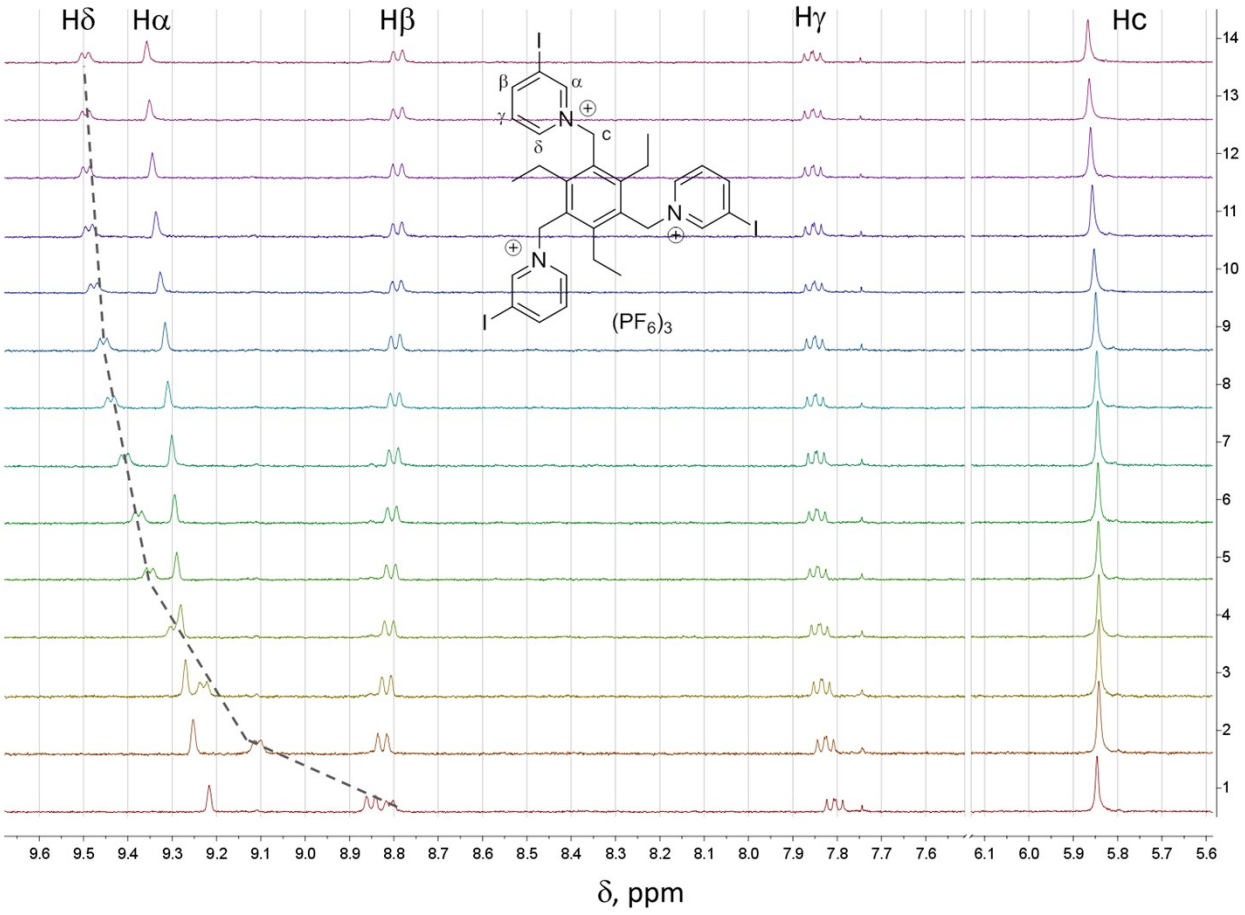

Fig. S15. ^{1}H-NMR spectra taken during the titration of **3**$(PF_6)_3$ (0.2 mM) with TBACl in CD_3CN/d^6-DMSO mixture (10% d^6-DMSO). See the manuscript for comments

6. Crystal structure of $2(NO_3)_2(PF_6)$

As for the crystal structure of **2**(Br)$(PF_6)_2$, the $\mathbf{2}^{3+}$ molecular cations display a "2-up, 1-down" configuration (Fig. S16). The motif of HB and XB interactions is similar to that observed for bromide. In particular, two C-H groups belonging to the "2-up" iodopyridinium arms act as H-donors towards two O atoms of the nitrate ion (H-acceptors) within the cavity. This anion also interacts with the C-I(2) XB-donor group of a second $\mathbf{2}^{3+}$ cation, thus originating supramolecular chains. In the solid, other two XB interactions can be found: (i) a strong C-I···O interaction (Table 4) between C-I(1) and O(3) of a second nitrate anion (XB-acceptor); (ii) a weak interaction involving C-I(3) and F(3) of a PF_6^- counter ion (XB-acceptor). Notice that the positional disorder occurring in the **2**$(NO_3)_2(PF_6)$ crystal affects the nitrate counter ion involved in the assembling of the supramolecular chain, therefore this species is not always present in the molecules forming the crystal.

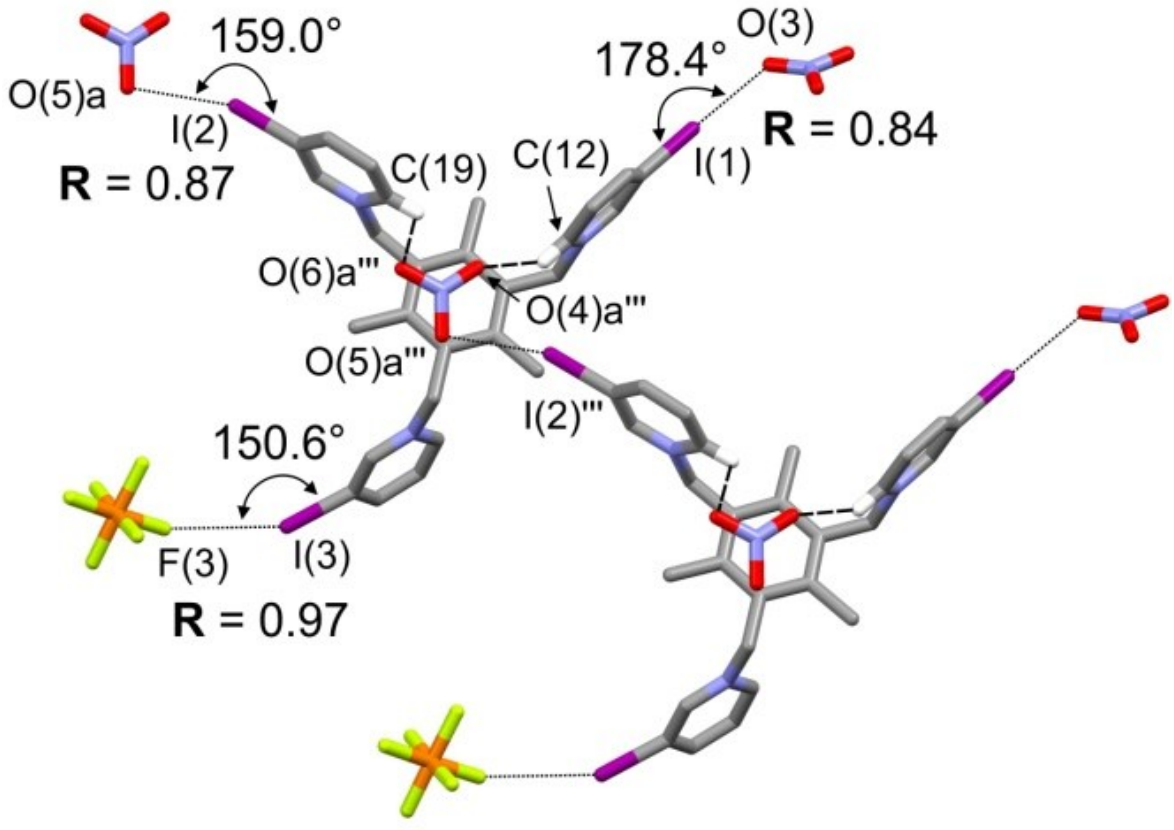

Fig. S16. A simplified sketch of the crystal structure of **2**$(NO_3)_2(PF_6)$. Names are shown only for atoms involved in C-I···Y halogen bonds (drawn with dotted lines), and weak C-H···A hydrogen bonds (drawn with dashed lines). The normalized **R** values = dI···Y/(rI+rY) and the C-I···Y bond angles are reported. Symmetry code: (") x, -1+y, z; (''') -1+x, y, z.

7. ORTEP images of 1a(PF_6), 1a(I), 2($(NO_3)_2$)(PF_6) and 2(Br)(PF_6)$_2$

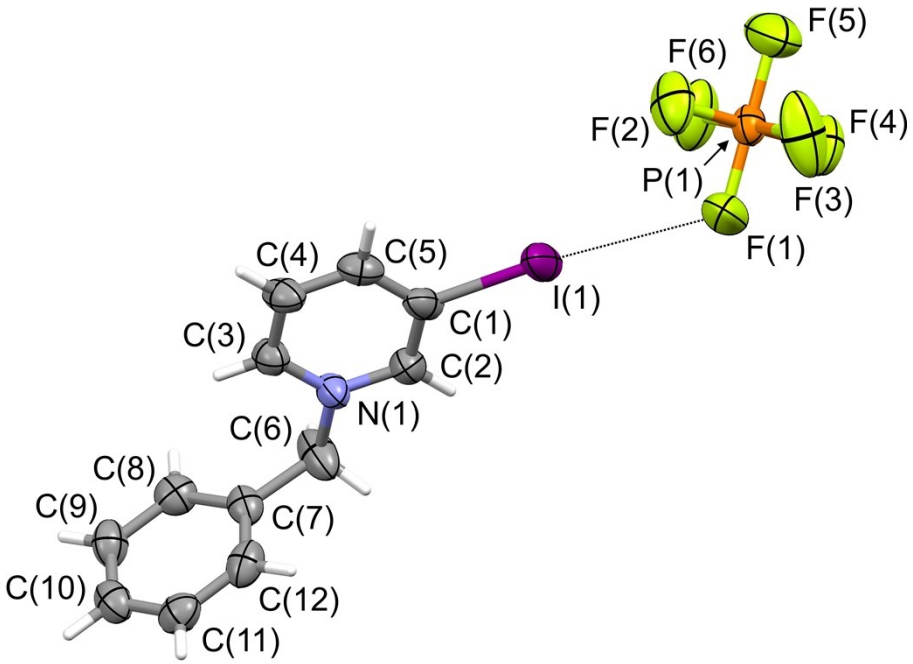

Fig. S17. Plot showing thermal ellipsoids of the asymmetric unit of the **1a**(PF_6) crystal salt (ellipsoids are drawn at the 30% probability level). An XB interaction is drawn with dotted line.

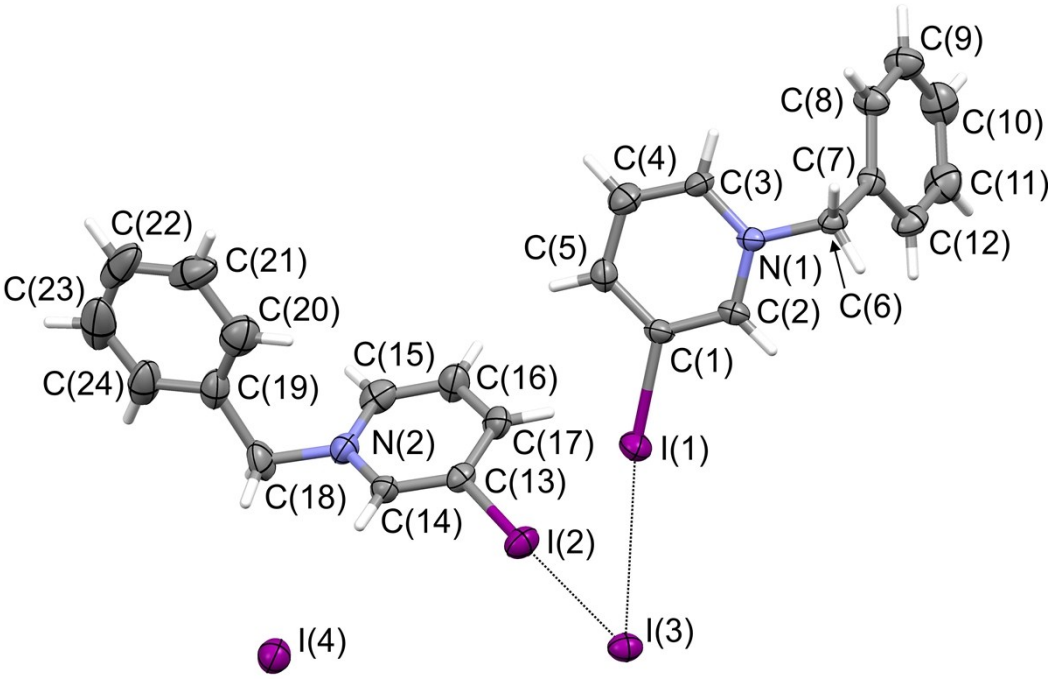

Fig. S18. Plot showing thermal ellipsoids of the asymmetric unit of the **1a**(I) crystal salt (ellipsoids are drawn at the 30% probability level). Two XB interactions are drawn with dotted line.

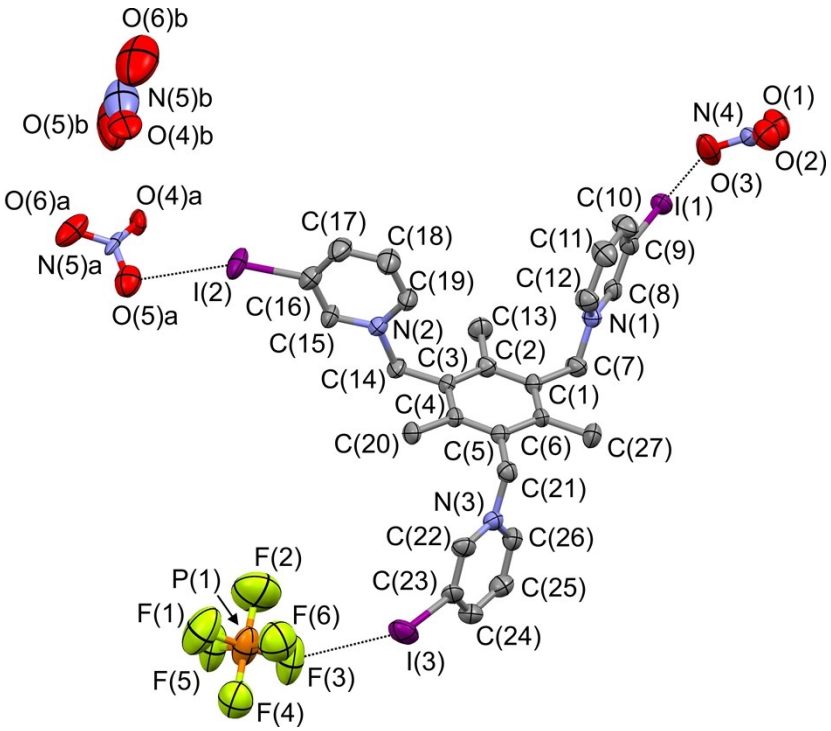

Fig. S19. Plot showing thermal ellipsoids of the asymmetric unit of the **2**$(NO_3)_2(PF_6)$ crystal salt (ellipsoids are drawn at the 30% probability level, hydrogens are omitted for clarity). Three XB interactions are drawn with dotted line. Nitrate atom positions with a and b suffix are mutually exclusive and half populated.

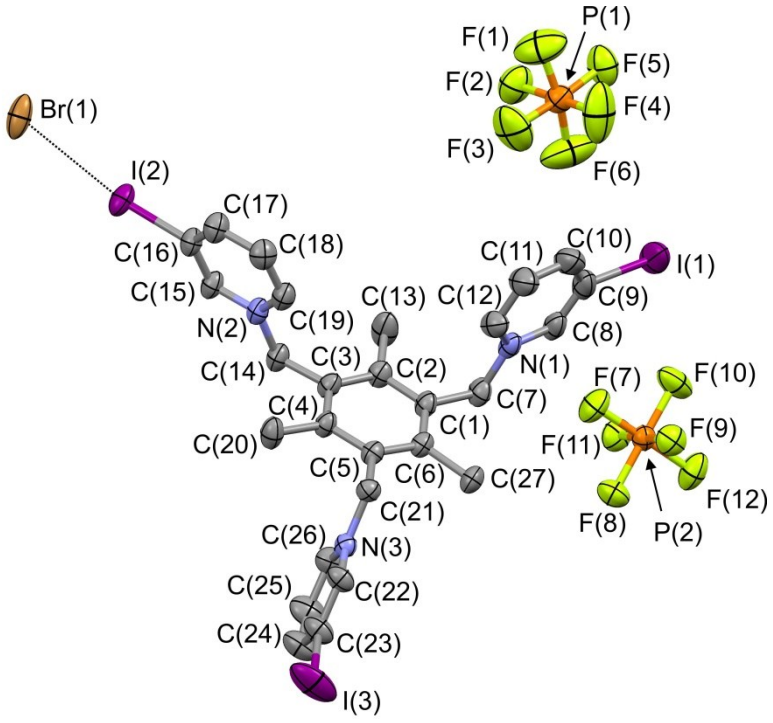

Fig. S20. Plot showing thermal ellipsoids of the asymmetric unit of the **2**$(Br)(PF_6)_2$ crystal salt (ellipsoids are drawn at the 30% probability level, hydrogens are omitted for clarity). An XB interaction is drawn with dotted line.

8. NMR spectra of 1a(PF_6), 2(PF_6)$_3$ and 3(PF_6)$_3$

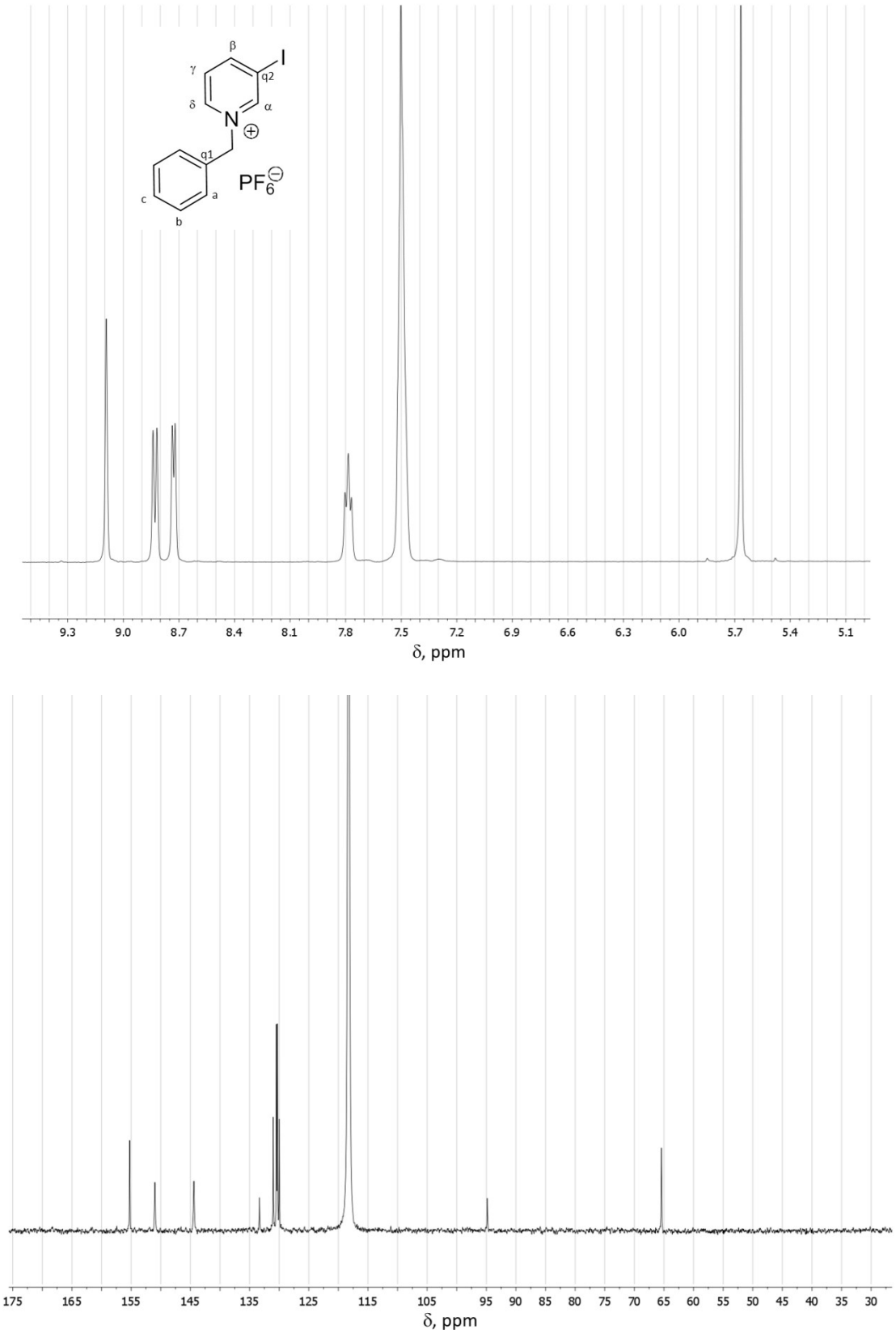

Fig. S21: ^{1}H and ^{13}C-NMR spectra of **1a**(PF_6) in CD_3CN

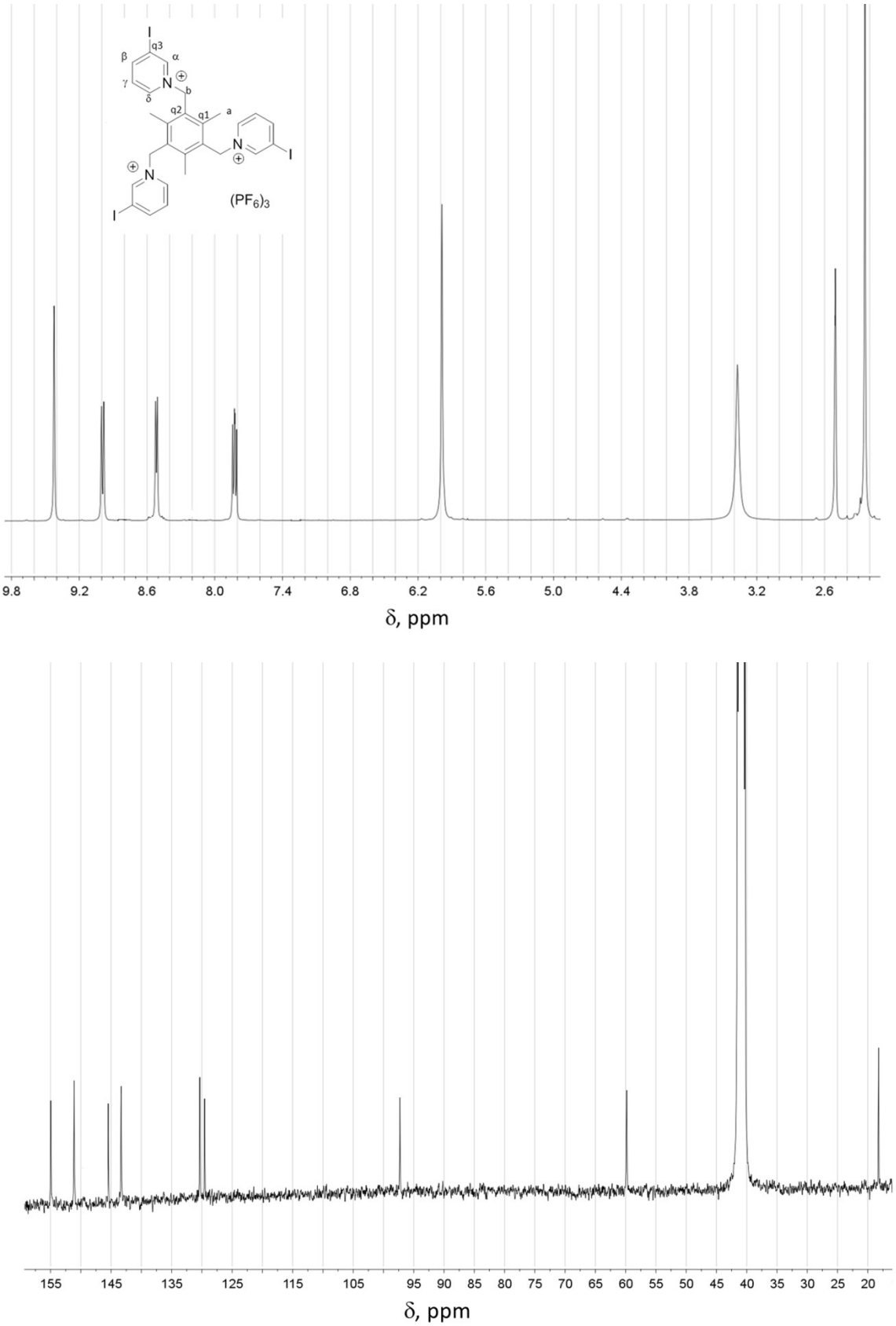

Fig. S22: ^{1}H and ^{13}C-NMR spectra of **2**$(PF_6)_3$ in d^6-DMSO

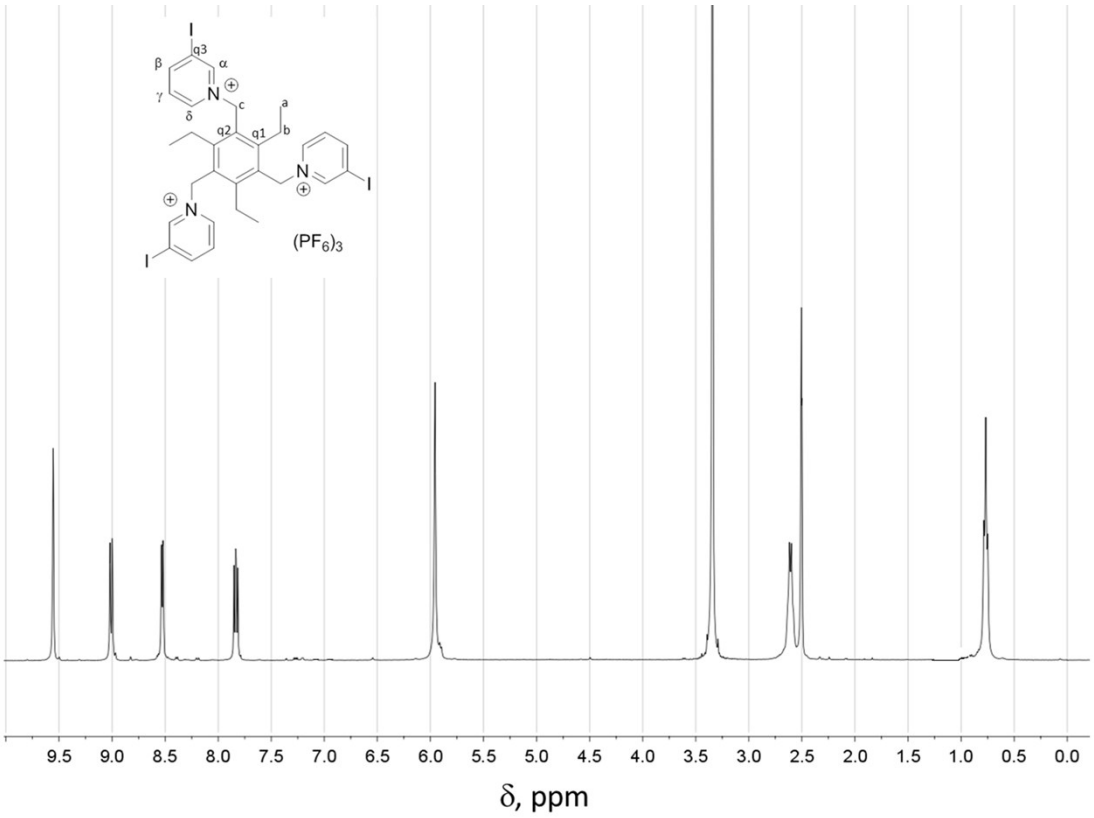

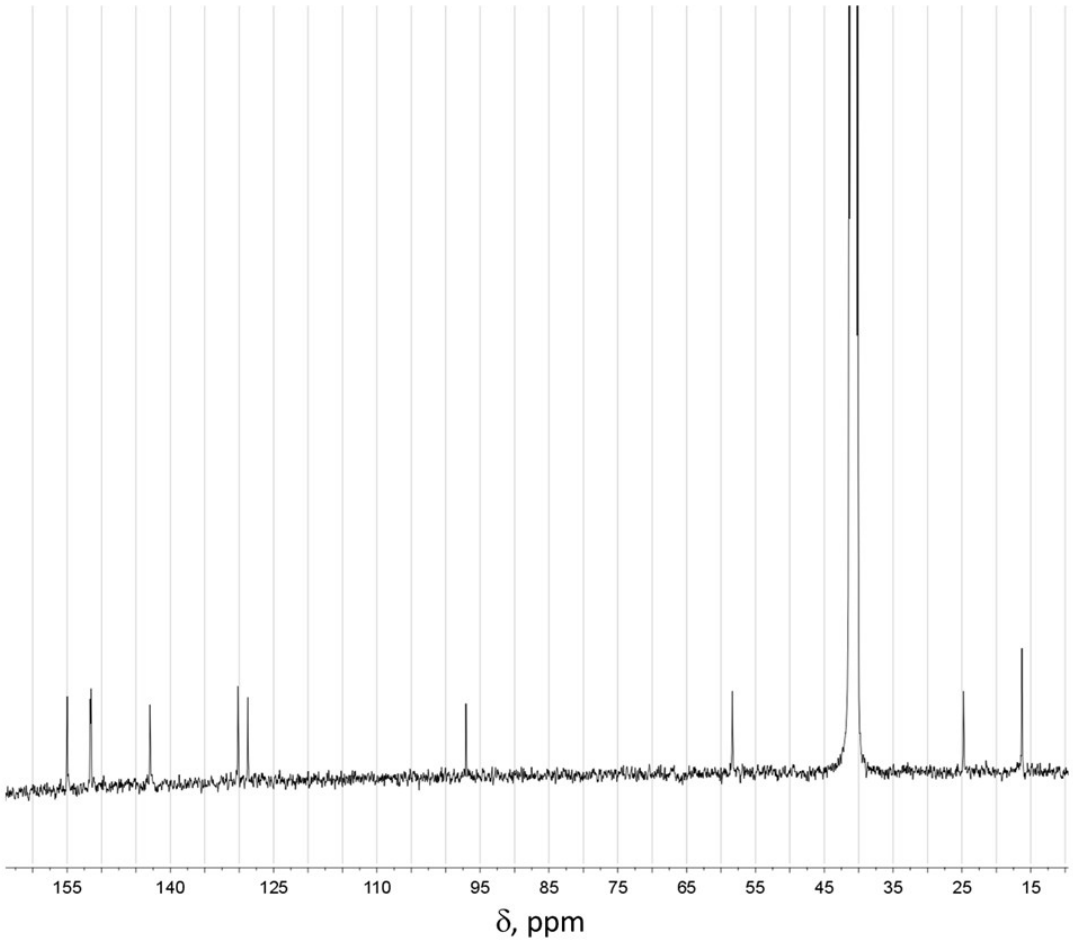

Fig. S23: ^{1}H and ^{13}C-NMR spectra of **3**$(PF_6)_3$ in d^6-DMSO

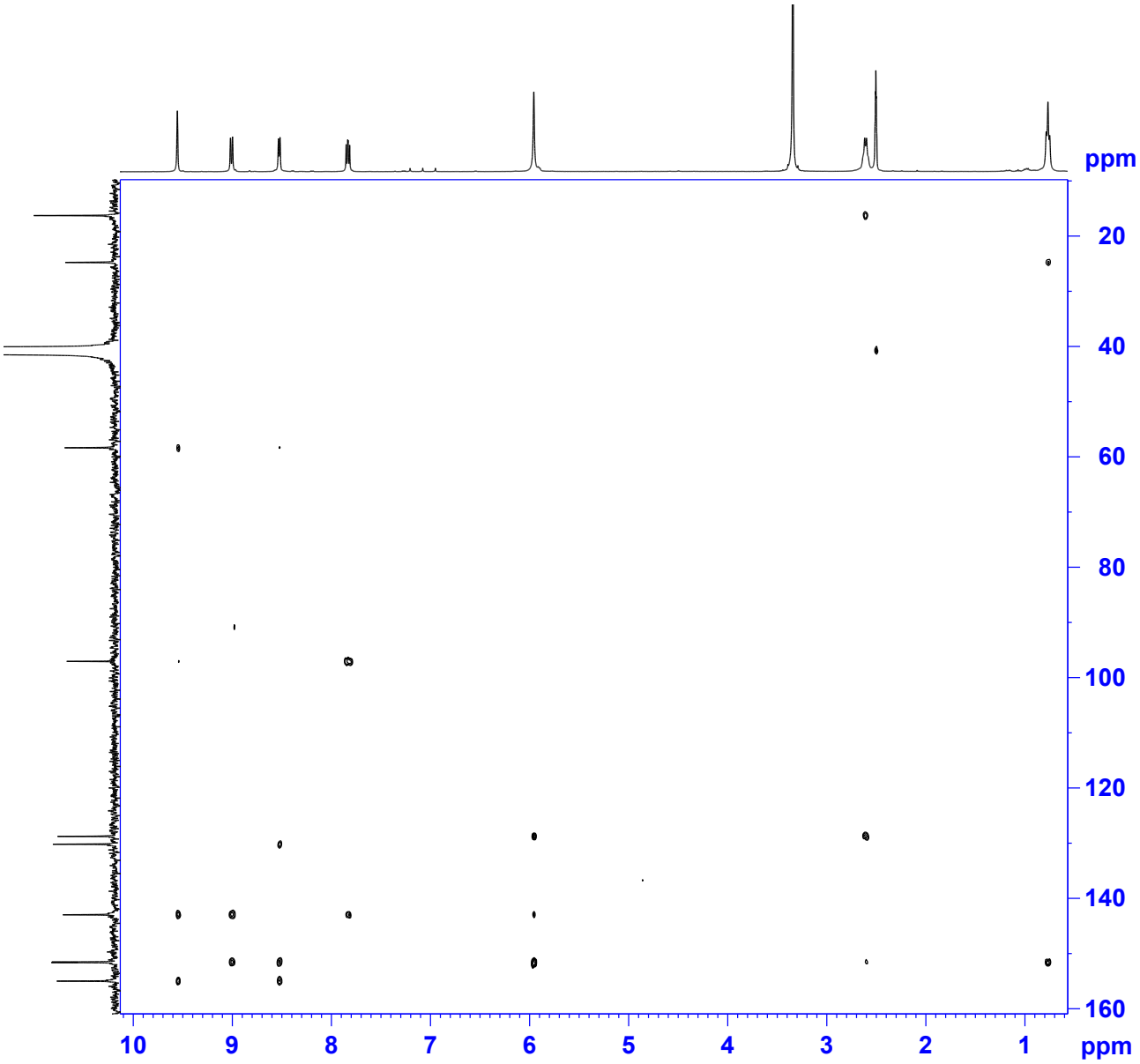

Fig. S24a: $^{1}H,^{13}C$-HMBC spectrum of **3**$(PF_6)_3$ in d^6-DMSO (full spectrum)

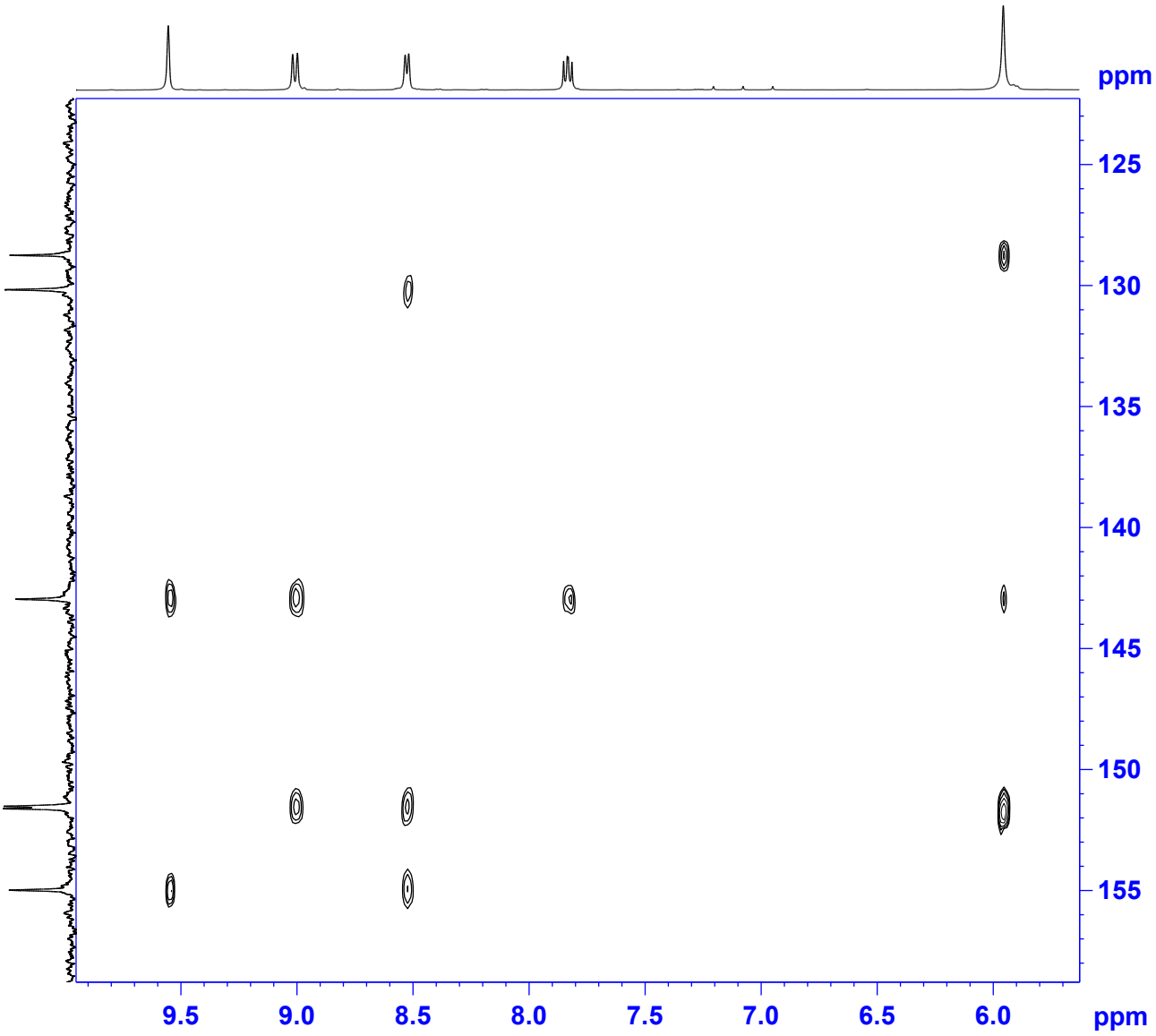

Fig. S24b: Detail of Fig. S20a: $\Delta\delta$ = 5.6- 9.9 ppm

References

1. A. Bondi, J Phys. Chem. 1964, 68, 441.

2. G.R. Desiraju, P.S. Ho, L. Kloo, A.C. Legon, R. Marquardt, P. Metrangolo, P.A. Politzer, G. Resnati, and K. Rissanen, Pure Appl. Chem., 2013, 85, 1711.